

## STRONG X-RAY ABSORPTION IN A BROAD ABSORPTION LINE QUASAR: PHL 5200

SMITA MATHUR<sup>1</sup> AND MARTIN ELVIS

Harvard-Smithsonian Center for Astrophysics, 60 Garden Street, Cambridge, MA 02138

AND

K. P. SINGH<sup>2</sup>

Laboratory for High Energy Astrophysics, Code 668, NASA/GSFC, Greenbelt, MD 20771

Received 1995 September 5; accepted 1995 September 26

### ABSTRACT

We present *ASCA* observations of the  $z = 1.98$  prototype broad absorption line quasar (BALQSO): PHL 5200. The source was detected in both SIS and GIS. A power-law spectrum ( $\alpha_E = 0.6^{+0.9}_{-0.6}$ ) with large intrinsic absorption ( $N_H = 1.3^{+2.3}_{-1.1} \times 10^{23} \text{ cm}^{-2}$ ) best describes the spectrum. Excess column density over the local Galactic value is required at the 99% confidence level. This detection suggests that, although BALQSOs are X-ray-quiet, it is strong absorption in the BAL region that makes them appear faint to low-energy X-ray experiments. The required intrinsic absorbing column density is 2–3 orders of magnitude larger than earlier estimates of column densities in BALQSOs. This implies that the BAL systems are much more highly ionized than was previously thought.

*Subject headings:* quasars: absorption lines — quasars: individual (PHL 5200) — X-rays: galaxies

### 1. INTRODUCTION

Associated absorption is common in the optical and ultraviolet spectra of quasars (Ulrich 1988). A subset of these have very broad absorption line profiles extending up to  $\Delta v = 0.1c$ – $0.2c$  redward with respect to the quasar rest frame (see, e.g., Turnshek 1988). These broad absorption line quasars (BALQSOs) show absorption features due to high-ionization lines of  $C^{+3}$ ,  $Si^{+3}$ , and other ions. Low-ionization BALQSOs have also been observed which show  $Mg^{+1}$  and/or  $Al^{+2}$  absorption troughs. BALQSOs have been estimated to have column densities  $N_H \sim 10^{20}$ – $10^{21} \text{ cm}^{-2}$  (Turnshek 1984; Hamann, Korista, & Morris 1993). As a class, BALQSOs share some common properties: they are always radio-quiet (Stocke et al. 1992), may have abundances 10–100 times solar (in their emission lines; Turnshek 1988, Hamann & Ferland 1993), and are X-ray-quiet (Green et al. 1995). Recent work suggests that BALQSOs are normal radio-quiet quasars seen from an unusual direction (Weymann et al. 1991; Hamann et al. 1993). In this case all radio-quiet quasars have collimated BAL outflows, which, however, are pointed out of our line of sight in some 90% of cases. Thus BALQSOs, far from being exotic objects, give us a special probe into the gasdynamics around the typical quasar.

However, physical conditions in the absorbing gas in the BALQSOs are poorly determined from optical/UV absorption-line studies (Lanzetta et al. 1991). This is because only a few, usually saturated, lines are measured, yielding lower limits to column densities for a few ions but little information on the ionization state. If, as in the narrow-line-associated absorbers, there is X-ray absorption as well as optical and UV, then the combined X-ray and UV analysis would allow us to derive the physical conditions in BALQSO absorption systems (Mathur et al. 1994; Mathur 1994; Mathur, Elvis, & Wilkes 1995). This, however, has been difficult, since BALQSOs are elusive X-ray

sources and so are otherwise essentially unconstrained in their X-ray properties. In a soft X-ray study of quasars with *Einstein*, only four out of nine BALQSOs were detected (Zamorani et al. 1981). Initial results from *ROSAT* are mainly upper limits (Kopko, Turnshek, & Espey 1993; Green et al. 1995), implying that they are relatively faint in soft X-rays (i.e., have steep  $\alpha_{ox}$ ). Our understanding of BALQSOs is incomplete without a knowledge of their X-ray properties. In fact, lack of knowledge of the underlying ionizing continuum is one of the major uncertainties in the models of BALQSOs: Are they intrinsically X-ray-quiet (i.e., large  $\alpha_{ox}$ )? Or is it strong absorption that makes them look faint?

PHL 5200, a prototype BALQSO at  $z = 1.98$  (Burbidge 1968), was detected in hard X-rays by the *EXOSAT* medium-energy (ME) experiment but not by the low-energy (LE) experiment (Singh, Westergaard, & Schnopper 1987). To obtain consistency between the *EXOSAT* ME and LE requires a column density of  $\geq 10^{22} \text{ atoms cm}^{-2}$ , making it an excellent candidate for examining the BAL region. We observed PHL 5200 with *ASCA* with this aim in mind. *Einstein* did not detect (Zamorani et al. 1981) and *ROSAT* has not observed PHL 5200.

### 2. *ASCA* OBSERVATIONS AND DATA ANALYSIS

*ASCA* (Tanaka et al. 1994) observed PHL 5200 on 1994 June 21 for a net exposure time of 17.7 ks (Table 1). *ASCA* has two solid-state imaging spectrometers (SIS0 and SIS1; Loevenstein & Isobe 1992) and two gas imaging spectrometers (GIS3 and GIS4; Ohashi et al. 1991). The SISs were operated in 2 CCD mode (see Fig. 1). The source was faint but was clearly detected in SIS0 and GIS3 (Fig. 1). The X-ray position from SIS0 is (J2000)  $22^h 28^m 26^s$ ,  $-5^\circ 18' 54''$ , 1.1' from the optical position (Schneider et al. 1992), consistent with the current satellite pointing uncertainties (Tanaka et al. 1994). The source was off-axis in SIS1 (where it lay close to the gap between two chips) and GIS2 and was not detected in either. This is consistent with the fact that the optical axes of

<sup>1</sup> smita@cfa.harvard.edu.

<sup>2</sup> NRC Senior Research Associate, on leave from Tata Institute of Fundamental Research, Bombay, India.

TABLE 1  
*ASCA* OBSERVATIONS OF PHL 5200

Instrument	Total Counts	Exposure (s)	Net Count Rate ( $s^{-1}$ )
SIS0 .....	513	16,587	$0.01 \pm 0.001$
GIS3 .....	505	16,788	$0.006 \pm 0.001$

telescopes containing SIS0 and GIS3 are much closer to each other than the others. No other sources were seen in any of the instruments to a level similar to the count rates of PHL 5200.

Data were extracted in a standard way using the FTOOLS and XSELECT software.<sup>3</sup> Standard screening criteria were used as recommended in the *ASCA* ABC guide: a greater than  $10^\circ$  bright Earth angle, and a cutoff rigidity greater than 6 GeV/c. Hot and flickering pixels were removed from the SIS data using XSELECT. All SIS events of grade 0, 2, 3, and 4 were accepted. Data of both faint and bright modes with high, medium, and low telemetry rates were combined. These data can be combined without any calibration compromises. The *ASCA* X-ray telescope has a broad point-spread function, and jittering of the spacecraft can appear on arcminute scales. To take this into account, source counts were extracted from a circular region of  $6'$  radius for GIS3 and from a  $4'$  radius for SIS0. The source was pointed at the center of chip 1 of SIS0, putting the bulk of its photons into just one chip. Detectors SIS0 and GIS3 yielded  $\sim 500$  total counts each. Data from these detectors cannot be combined, since the detectors have different properties. The background was estimated using the same spatial filter on the deep field background images (*ASCA* ABC guide). A background-subtracted count rate of  $(1.04 \pm 0.15) \times 10^{-2}$  was observed by SIS0, and  $(6.26 \pm 1.47) \times 10^{-3}$  by GIS3. The data were grouped to contain at least 10 counts (background-subtracted) per pulse-height analysis (PHA) channel to allow the use of the Gaussian statistic. The data have modest signal-to-noise ratio; however, it can be clearly seen that there are essentially no counts below  $\sim 1$  keV ( $\sim 3$  keV in the rest frame) (see Fig. 2). The highest rest energy

<sup>3</sup> FTOOLS is a collection of utility programs to create, examine, or modify data files in FITS format. XSELECT is a command-line interface to the FTOOLS, for X-ray astrophysical analysis. The software is distributed by the *ASCA* Guest Observer Facility.

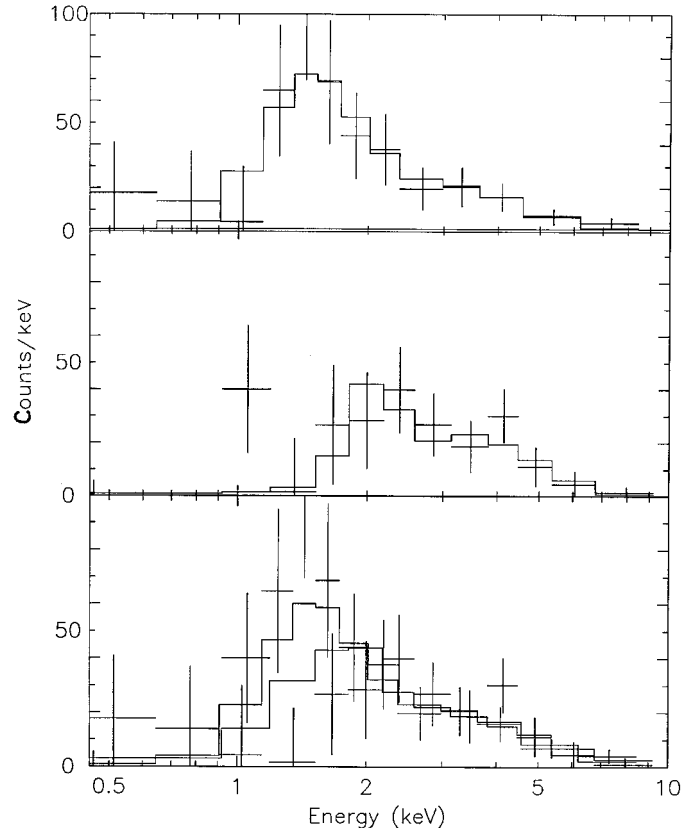


FIG. 2.—*ASCA* spectral data (crosses) with best-fit power law with fixed Galactic and intrinsic absorption models. Top: SIS; middle: GIS; bottom: both SIS and GIS.

detected for PHL 5200 is 12 keV at  $3\sigma$  for 0.5 keV wide bins. Figure 2 shows the SIS and GIS spectra of PHL 5200.

The SIS and GIS spectra extracted in this way were then analyzed using XSPEC. The 1995 March release of the response matrices was used for the GIS data, and the 1994 November release for the SIS data. A power-law spectrum with fixed Galactic absorption ( $4.8 \times 10^{20}$  atoms  $cm^{-2}$ ; Stark

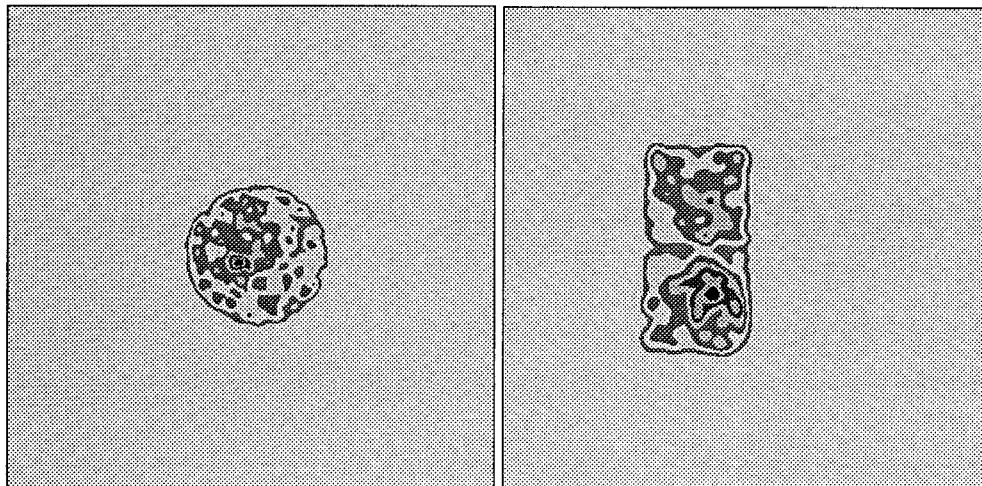


FIG. 1.—*ASCA* GIS3 (left) and SIS0 (right) gray-scale images around PHL 5200. North is  $66^\circ 7'$  clockwise from the top. The GIS field of view is  $50'$  in diameter, and each SIS chip is  $11.1'$  on a side (*ASCA* Technical Description 1993).

TABLE 2  
SPECTRAL FITS TO *ASCA* DATA OF PHL 5200

Model	$\alpha_E$	$N_H$ (free) <sup>a</sup>	Normalization <sup>b</sup>	$\chi^2$ (dof) <sup>c</sup>
SIS				
Power law:				
+ $N_H$ .....	$0.9^{+1.3}_{-1.0}$	$0.9^{+1.2}_{-0.8}$	$1.3^{+4.8}_{-0.3}$	5.2 (12)
+ $N_H$ (Galactic) fixed.....	$-0.1^{+0.4}_{-0.4}$	...	$0.3^{+0.1}_{-0.2}$	8.4 (13)
+ $N_H(z = 1.98)$ .....	$0.8^{+1.1}_{-0.9}$	$14.0^{+19.7}_{-12.4}$	$1.2^{+3.4}_{-0.4}$	4.8 (12)
GIS				
Power law:				
+ $N_H$ .....	$2.0^{+3.1}_{-1.8}$	$4.5^{+0.0}_{-3.8}$	$9.6^{+875}_{-0.5}$	5.4 (9)
+ $N_H$ (Galactic) fixed.....	$-0.1^{+0.5}_{-0.6}$	...	$0.3^{+0.2}_{-0.1}$	9.8 (10)
+ $N_H(z = 1.98)$ .....	$2.8^{+6.2}_{-2.6}$	$130^{+0}_{-118}$	$47^{+170}_{-0.5}$	5.7 (9)
SIS + GIS				
Power law:				
+ $N_H$ .....	$0.6^{+0.0}_{-0.7}$	$0.9^{+1.4}_{-0.7}$	$1.0^{+2.9}_{-0.4}$	14.1 (24)
+ $N_H$ (Galactic) fixed.....	$-0.1^{+0.3}_{-0.3}$	...	$0.3^{+0.1}_{-0.2}$	18.4 (25)
+ $N_H(z = 1.98)$ .....	$0.6^{+0.9}_{-0.6}$	$13.1^{+23.2}_{-11.1}$	$0.9^{+3.0}_{-0.4}$	14.2 (24)

<sup>a</sup> Times  $10^{22} \text{ cm}^{-2}$ .

<sup>b</sup> In units of  $10^{-4} \text{ photons keV}^{-1} \text{ cm}^{-2} \text{ s}^{-1}$  at 1 keV.

<sup>c</sup> Degrees of freedom in parentheses.

et al. 1992) provides an acceptable fit to the SIS0 data (Table 2). However, if absorption is allowed to be a free parameter, then the fit is improved with greater than 98% confidence ( $F$ -test; Table 2). The fitted value [ $N_H(z = 0) = 9 \times 10^{21} \text{ atoms cm}^{-2}$ ; solar abundance] is much larger than the Galactic column density toward PHL 5200, indicating excess absorption along the line of sight. This is also much larger than the uncertainties in the SIS low-energy response, which may overestimate the column density by up to  $2 \times 10^{20} \text{ cm}^{-2}$  (C. S. R. Day, Calibration Uncertainties [1995], *ASCA* GOF WWW page [URL: [http://heasarc.gsfc.nasa.gov/docs/asca/cal\\_probs.html](http://heasarc.gsfc.nasa.gov/docs/asca/cal_probs.html)]). We then fitted a power-law spectrum with Galactic column and an additional column of absorber allowing its redshift to be free. We found no preferred redshift for the additional absorber. Fixing the absorber at the source gives a column density of  $1.4^{+2.0}_{-1.2} \times 10^{23} \text{ cm}^{-2}$  (90% confidence for one parameter; solar abundance). The power-law energy index is  $\alpha_E = 0.8^{+1.1}_{-0.9}$ .

For the GIS data, a similar fit of a power-law spectrum with fixed Galactic and additional  $z = 1.98$  absorption is acceptable but does not constrain the parameters well because the data have large errors (Table 2).

A combined SIS and GIS analysis does constrain the parameters of the model slightly better (Fig. 3; Table 2). The column density at the source is  $1.3^{+2.3}_{-1.1} \times 10^{23} \text{ cm}^{-2}$ , and  $\alpha_E = 0.6^{+0.9}_{-0.6}$ . This excess absorption, above Galactic  $N_H$ , is required at 99% confidence ( $F$ -test).

The 2–10 keV (observed frame) flux is  $2.9^{+13.9}_{-1.3} \times 10^{-13} \text{ ergs s}^{-1} \text{ cm}^{-2}$  (corrected for best-fit absorption), and a 2–10 keV (rest frame) luminosity is  $9.3 \times 10^{45} \text{ ergs s}^{-1}$  ( $H_0 = 50, q_0 = 0$ ). The flux in the *EXOSAT* ME band (2–6 keV observed) is  $2^{+6}_{-1} \times 10^{-13} \text{ ergs s}^{-1} \text{ cm}^{-2}$ . This is smaller than the *EXOSAT* flux ( $\sim 2 \times 10^{-12} \text{ ergs s}^{-1} \text{ cm}^{-2}$ ; Singh et al. 1987) by at least a factor of 2.5. The optical continuum of PHL 5200 does not

vary by such a large amount (Barbieri, Romano, & Zambon 1978). It is possible that it is variable absorption rather than intrinsic source variability that might be responsible for the difference in the *ASCA* and *EXOSAT* ME fluxes. The *ASCA* flux is consistent with the upper limits observed by the *Einstein* IPC (less than  $4.5 \times 10^{-13} \text{ ergs s}^{-1} \text{ cm}^{-2}$ ) and the *EXOSAT* CMA (less than  $5 \times 10^{-13} \text{ ergs s}^{-1} \text{ cm}^{-2}$ ).

The *ASCA*-derived monochromatic luminosity at 2 keV

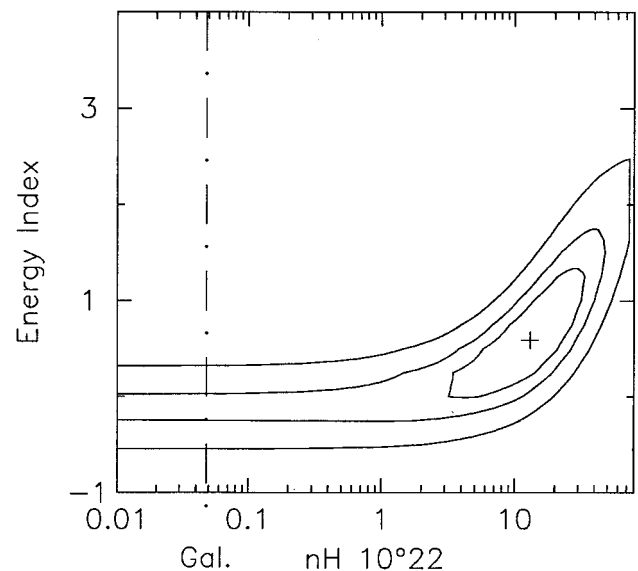


FIG. 3.—Confidence contours for the combined SIS and GIS spectrum. Contours of 68%, 90%, and 99% confidence regions are shown. The Galactic column density is shown as a dot-dashed line.

(rest frame) is  $1.3 \times 10^{28}$  ergs  $s^{-1}$  Hz $^{-1}$ , and at 2500 Å (rest frame) it is  $1.2 \times 10^{32}$  ergs  $s^{-1}$  Hz $^{-1}$  (Zamorani et al. 1981), giving  $\alpha_{ox} = 1.5$ .

An Fe K absorption edge is not detected ( $\tau < 0.9$ ; 90% confidence for one interesting parameter). The opacity of an Fe edge corresponding to  $N_H = 10^{23}$  cm $^{-2}$  is  $\tau = 0.1f_{ion}$ , where  $f_{ion}$  is the ionization fraction of iron in hydrogen-like state. Our data are not sensitive enough to detect such an edge.

The Fe K emission line (Ross & Fabian 1993) is also not detected (see Fig. 2). We place a 0.5 keV upper limit (90% confidence for one interesting parameter) to the rest-frame equivalent width of a narrow ( $\sigma < 10$  eV) line between 2.1 and 2.4 keV (6.3–7.1 keV rest frame). This can be used to place an upper limit on the covering factor of the absorber. If the absorber is a uniform spherical shell surrounding the X-ray continuum source, then the Fe K $\alpha$  line flux through recombination after photoionization of helium-like iron is given by  $I_{line} = [N_H A(Fe)/10^{19.8}] (\Omega/4\pi) I_{abs} \eta$  (Basko 1980), where  $\eta$  is the fluorescent yield, the efficiency with which the flux above 7.1 keV ( $I_{abs}$ ) is reemitted as an Fe K line. Assuming solar abundance of iron [ $A(Fe) = 3.3 \times 10^{-5}$ ; Grevesse & Andres 1989] and  $\eta = 0.5$  (Krolik & Kallman, 1987), we estimate the covering factor of the line emitting region,  $\Omega/4\pi < 4f_{ion}^{-1}$ , which is not an interesting limit. If, however, the heavy-element abundance is 10 times solar (Hamann & Ferland 1993), then  $\Omega/4\pi < 0.4f_{ion}^{-1}$ , consistent with Hamann et al. (1993).

### 3. DISCUSSION

The *ASCA* spectrum of PHL 5200 shows excess absorption at 99% confidence. A column density of  $(0.2-4) \times 10^{23} (Z_{\odot}/Z)$  cm $^{-2}$  is obtained if the absorber is at the source. A power law was a good fit to the data with the spectral slope ( $\alpha_E = 0.6_{-0.6}^{+0.9}$ ) in the normal range (Wilkes et al. 1994). The PHL 5200 value of  $\alpha_{ox} = 1.5$  is also normal for a radio-quiet quasar (Wilkes et al. 1994).

The inferred absorbing column density for PHL 5200 is 2–3 orders of magnitude larger than the earlier estimates of column density in BALQSOs (Hamann et al. 1993; Turnshek 1984). This implies that the BAL clouds may be more highly ionized ( $N_H/N_H \sim 10^{-8}$ ) than previously thought ( $N_H/N_H \sim 10^{-5}$ ; Hamann et al. 1993), as was true with narrow associated absorbers (Mathur et al. 1994, 1995). The estimates from

the saturated UV lines appear to have been misleading. Recent models of BALQSOs (Murray et al. 1995), however, do consider column densities as large as we find in PHL 5200. If, on the other hand, the abundances are 100–1000 times solar, then the hydrogen column density would be smaller ( $N_H \sim 10^{20}$  cm $^{-2}$ ). However, the ionization state would still be high, since the comparison is between metal line absorption in the UV and absorption in X-rays. The column density in PHL 5200 is also about an order of magnitude larger than other, narrow, associated absorption systems (Fiore et al. 1993; Turner et al. 1994). In this respect, as in velocity width, the BALQSOs may be extreme examples of other associated absorbers.

This is consistent with our earlier conjecture that all associated absorbers may form a continuum of properties with column density, outflow velocity, and the distance from the central continuum (Mathur et al. 1994). Are BALQSOs also similar to these in being “XUV absorbers,” i.e., are the broad absorption lines observed in the UV caused by the same matter producing X-ray absorption? This can be investigated by combined analysis of X-ray and UV spectra (Mathur et al. 1994, 1995) of PHL 5200 but is beyond the scope of this paper. If they are indeed the same, it would allow us to further constrain the physical properties of the absorber and so of the outflowing circumnuclear matter (Mathur et al. 1995).

The present study implies that BALQSOs are not intrinsically X-ray quiet; it is the extreme absorption that makes them appear faint to low-energy experiments. Since the absorption is significant only in soft X-rays, hard X-ray observations, above a few keV, would reveal their presence as X-ray sources. This can be done with missions like *ASCA*, *XTE*, *SAX*, and *AXAF*. We have been awarded *XTE* time to observe BALQSOs with this aim.

This research has made use of the NASA/IPAC Extragalactic Database (NED), which is operated by the Jet Propulsion Laboratory, Caltech, under contract with the National Aeronautics and Space Administration. This work was supported by NASA grants NAGW-2201 (LTSA), NAG5-2563 (ASCA), NAGW-4490 (LTSA), and NASA contract NAS8-39073 (ASC).

### REFERENCES

- Barbieri, C., Romano, G., & Zambon, M. 1978, *A&AS*, 31, 401  
 Basko, M. M. 1980, *A&A*, 87, 330  
 Burbidge, E. M. 1968, *ApJ*, 152, 111  
 Fiore, F., Elvis, M., Mathur, S., & Wilkes, B. 1993, *ApJ*, 415, 129  
 Green, P. J., et al. 1995, *ApJ*, 450, 51  
 Grevesse, N., & Andres, E. 1989, in *AIP Conf. Proc.* 183, *Cosmic Abundances of Matter*, ed. C. J. Waddington (New York: AIP), 1  
 Hamann, F., & Ferland, G. 1993, *ApJ*, 418, 11  
 Hamann, F., Korista, K., & Morris, S. L. 1993, *ApJ*, 415, 541  
 Kopko, M., Turnshek, D. A., & Espey, B. 1993, in *IAU Symp.* 159, *Quasars across the Electromagnetic Spectrum* ed. T. J.-L. Courvoisier & A. Blench (Dordrecht: Kluwer), 450  
 Krolik, J. H., & Kallman, T. R. 1987, *ApJ*, 320, L5  
 Lanzetta, K. M., Wolfe, A. M., Turnshek, D. A., Lu, L., McMahon, R. G., & Hazard, C. 1991, *ApJS*, 77, 1  
 Loewenstein, T., & Isobe, T. 1992, translation of *ASCA Interim Rep.*, ISAS  
 Mathur, S. 1994, *ApJ*, 431, L75  
 Mathur, S., Elvis, M., & Wilkes, B. 1995, *ApJ*, 452, 230  
 Mathur, S., Wilkes, B., Elvis, M., & Fiore, F. 1994, *ApJ*, 434, 493  
 Murray, N., Chiang, J., Grossman, S. A., & Voit, G. M. 1995, *ApJ*, 451, 498  
 Ohashi, T., et al. 1991, *Proc. SPIE*, 1549, 9  
 Ross, R. R., & Fabian, A. C. 1989, *MNRAS*, 261, 74  
 Schneider, D. P., et al. 1992, *PASP*, 104, 678  
 Singh, K. P., Westergaard, N. J., & Schnopper, H. W. 1987, *A&A*, 172, L11  
 Stark, A. A., Gammie, C. F., Wilson, R. W., Bally, J., Linke, R., Heiles, C., & Hurwitz, M. 1992, *ApJS*, 79, 77  
 Stocke, J. T., Morris, S. L., Weymann, R. J., & Foltz, C. B. 1992, *ApJ*, 396, 487  
 Tanaka, Y., Holt, S. S., & Inoue, H. 1994, *PASJ*, 46, L37  
 Turner, T. J., Nandra, K., George, I. M., Fabian, A., & Pounds, K. A. 1994, *ApJ*, 419, 127  
 Turnshek, D. A. 1984, *ApJ*, 280, 51  
 ———. 1988, in *QSO Absorption Lines: Probing the Universe*, ed. J. C. Blades, D. Turnshek, & C. Norman (Cambridge: Cambridge Univ. Press), 17  
 Ulrich, M. H. 1988, *MNRAS*, 230, 121  
 Weymann, R., Morris, S. L., Foltz, C. B., & Hewett, P. C. 1991, *ApJ*, 373, 23  
 Wilkes, B. J., Tananbaum, H., Worrall, D. M., Avni, Y., Oey, M. S., & Flanagan, J. 1994, *ApJS*, 92, 53  
 Zamorani, G., et al. 1981, *ApJ*, 245, 357